Petroleum Science 19 (2022) 3059–3067

Contents lists available at ScienceDirect

Petroleum Science

journal homepage: www.keaipublishing.com/en/journals/petroleum-science

Original Paper

An approximate analytical solution for transient gas flows in a vertically fractured well of finite fracture conductivity

Yun-Hu Lu [a, *], Kang-Ping Chen [b], Yan Jin [a], Hong-Da Li [a], Quan Xie [c]

[a] College of Petroleum Engineering, China University of Petroleum (Beijing), Beijing, 102200, China
[b] School for Engineering of Matter, Transport and Energy, Arizona State University, Tempe, AZ, 85287-6106, USA
[c] Discipline of Petroleum Engineering, WA School of Mines: Minerals, Energy and Chemical Engineering, Curtin University, 26 Dick Perry Avenue, 6151, Kensington, Western Australia, Australia

ARTICLE INFO

Article history:
Received 14 January 2022
Received in revised form
5 May 2022
Accepted 5 May 2022
Available online 7 May 2022

Edited by Xiu-Qiu Peng

Keywords:
Transient gas pressure
Fractured well
Analytical solution

ABSTRACT

An analytical solution in physical variable space is presented for transient gas flows during constant-rate production from a vertically-fractured well in an infinite homogeneous reservoir with finite fracture conductivity. The solution is based on the short-time asymptotic solution and a new approximate transient elliptical flow solution, which covers transient flows from the bilinear flow regime to the pseudo-radial flow regime. The solution covers the well-known asymptotic solutions in both short- and long-time limits of bilinear and pseudo-radial flows. The analytical model provides a practical and reliable engineering tool to evaluate the fractured reservoir properties, which can be programmed using a spreadsheet.

1. Introduction

Hydraulic fracturing is important for the development of the tight gas and unconventional shale gas reservoirs. After the completion of the hydraulic fracturing, large quantities of propents would be needed to keep the fractures open, allowing hydrocarbon gas to flow from the reservoir to the fractures, and on to the wellbore and surface facilities. In this process, it is important to evaluate the conductivity of the fractures. Transient flow from vertically fractured wells is essential for estimating fractured reservoir properties (Agarwal et al., 1979; Agarwal, 1980; Baker and Ramey, 1978; Biryukov and Kuchuk, 2012; Cinco-Ley and Meng, 1988; Gringarten et al., 1975; Kuchuk and Habashy, 1997; Lee and Holditch, 1981; Raghavan, 1977; Rushing and Blasingame, 2003; Russell and Truitt, 1964; Valko and Economides, 1997; Wattenbarger and Ramey, 1969; Wilkinson, 1989), mostly for short- and intermediate-times as a pressure transient analysis. One of the best-known models for such vertically fractured wells is the finite conductivity fracture model developed by Cinco-Ley and collaborators (Cinco-Ley et al., 1978; Cinco-Ley and Samaniego, 1981). Cinco-Ley (Cinco-Ley et al., 1978) numerically solved an integral equation to obtain the well pressure response for constant-rate production; while Cinco-Ley and Samaniego (1981) analyzed a simplified model and identified flow regimes such as fracture linear flow, bilinear flow, formation linear flow, transient elliptical flow and pseudo-radial flow, which are useful for extracting petrophysical properties. Chen et al., (2016) applied numerical inversion to solve the transient pressure solution of the mathematical model. Tian et al., (2018) presented a new approximate semi-analytical method for predicting performance of a finite conductivity vertical fractured gas well produced at a variable production system. Zhang et al., (2018) developed a semi-analytical model to describe the pressure behavior of a vertical well with fishbone fracture pattern. And it is found that there are five flow regimes, they are bilinear flow, flow feed, fracture linear flow, formation linear flow, bi-radial flow and pseudoradial flow. Jiang et al., (2019) presented a composite elliptical flow model to analyse the fractured vertical well transient pressure and rate performance in TMGR with SRV and they applied Modified Mathieu functions to solve the mathematical model. Composite pressure transient responses model was developed to examine transient pressure behavior of a fractured vertical well with complex hydraulic and natural fracture networks by taking stress-sensitive effect into account (Jiang et al., 2020; Wang et al., 2017).

* Corresponding author.
E-mail address: luyunhu20021768@163.com (Y.-H. Lu).

https://doi.org/10.1016/j.petsci.2022.05.001

Nomenclatures

c_t	Total compressibility of the reservoir; 1/Pa
$C_{fD} = k_f w_f/(kL)$	Dimensionless fracture conductivity
$F_E = k_f w_f/(kL)$	Dimensionless elliptical fracture conductivity
h	Formation thickness; m
L	Ellipse focal distance/fracture half-length; m
$P_{i,d}$	Initial fluid pressure in the reservoir; Pa
$P_D = P_d/p_{i,d}$	Dimensionless fluid pressure in the reservoir
$\Delta P = P_{i,d} - P_{w,d}$	Well pressure drawdown; Pa
$P_{wD} = \frac{2\pi kh\Delta P}{\mu q_d}$	Dimensionless wellbore pressure drawdown
q_d	Production rate of the fractured well; m^3/s
$q_D = \frac{\mu q_d}{2\pi kh\Delta P}$	Dimensionless production rate of the fractured well
r_w	Wellbore radius; m
$t_{DL} = kt/(\mu\varphi c_t L^2)$	Dimensionless time based on fracture length
x, y	Cartesian coordinates; m
w_f	Fracture width at the wellbore; m
ξ, η	Elliptical coordinates; dimensionless
ξ_1	Elliptical fracture shape $\xi = \xi_1$
ξ_e	Elliptical reservoir shape $\xi = \xi_e$
k	Reservoir permeability; m^2
k_f	Fracture permeability; m^2
μ	Fluid viscosity; Pa·s
φ	Reservoir porosity; dimensionless

Studies have shown that an elliptical shape provides a good geometrical approximation to a hydraulic fracture, which offers certain advantages when it comes to finding the fluid production rate (Amini et al., 2007; Blasingame, 2008; Chen, 2016; Hale and Evers, 1981; Kucuk and Brigham, 1979; Lu and Chen, 2016; Obut and Ertekin, 1987; Prats et al., 1962; Riley, 1991; Riley et al., 1991; Sun et al., 2017; Zhang et al., 2011). For an elliptical fracture with an infinite fracture conductivity, Prats and Kucuk & Brigham (Kucuk and Brigham, 1979; Prats et al., 1962) obtained the well pressure for constant-rate fluid production. NGUYEN et al., 2020 proposed a straightforward semi-analytical solution for transient pressure behavior of multi-fractured horizontal gas wells producing from finite-conductivity fractures. But the proposed solution is developed based on coupling the solutions of two contiguous flow domains—matrix and fracture—both of which exhibit one-dimensional Cartesian flow. For finite fracture conductivity, Riley (Riley, 1991; Riley et al., 1991) carried out a comprehensive analytical study on the transient well pressure behavior for constant-rate production in an infinitely large reservoir, focusing on the exact analytical solution in the Laplace transform space ("semi-analytical solution"). However, given that pseudo-steady-state solution also includes the boundary effect, it is inappropriate to use a pseudo-steady-state solution to construct an approximation to the transient elliptical flow. To investigate the pressure transient behavior of the non-Darcy flow in composite naturally fractured-homogeneous gas reservoirs, Nie et al., (2021) developed a radial bi-zonal composite non-Darcy flow model based on Izbash's Equation. In addition, the mathematical models obtained above all require complex numerical solutions.

To the best of our knowledge, to date, there is no continuous, practical analytical solution in real-time space available for transient flow for a vertically fractured well at finite fracture conductivity. Such an easy-to-use explicit analytical solution in real-time space is highly desirable, as it can provide a practical tool to estimate gas well productivity in shale and tight gas reservoirs after the hydraulic fracturing (Poston and Poe, 2008).

The objective of the present paper is to fill this gap and to seek such an approximate analytical solution in the real-time space for transient fluid production from a fully-penetrated elliptical-shape vertical fracture in an infinite reservoir. It is noted that it is inappropriate to use a pseudo-steady-state solution to construct an approximation to the transient elliptical flow as a pseudo-steady-state solution also includes the boundary effect. The approximate solution proposed here is not intended to replace the existing numerical simulation tools; rather it serves as an alternative: using the derived formula allowing fast computations for additional desired data point as well as a reliable engineering tool for rapid evaluation of the transient well pressure in a first attempt to tackle such a problem. The reported formula can be programed in a spread sheet such as Excel, even on a hand-held calculator. The new analytical transient flow solution presented in this paper is obtained by patching the short-time asymptotic solution of Jin et al., (2015a) with a new approximate transient elliptical flow solution to be constructed below. This new composite solution is valid for finite fracture conductivity and it covers nearly all flow regimes occurring in an unbounded reservoir, from the early-time bilinear flow to the late-time pseudo-radial flow. The solution recovers exactly to the well-known asymptotic solutions in both the short-time bilinear flow limit and the long-time pseudo-radial flow limit. Moreover, this analytical model is also fully validated by the well-documented numerical results from Riley (Riley, 1991; Riley et al., 1991).

2. Methods and mathematical modeling

In this section, we briefly describe the asymptotic solution in short-times for constant rate production given by Jin (Jin et al., 2015a, 2015b), which will be used in constructing the new composite solution.

Fig. 1 shows the production from a fully-penetrated vertically-fractured well. To derive the analytical model, the following assumptions are made: (1) the reservoir fluid is a single-phase fluid residing in a homogeneous medium with its motion governed by Darcy's law in both the reservoir and the fracture; (2) the fluid and the reservoir are weakly compressible, characterized by a single lumped total compressibility constant c_t; (3) the effects of wellbore storage and skin are negligible; and (4) the hydraulic fracture is supported by propants and it can be considered as incompressible. The vertical hydraulic fracture is modeled as a thin, long ellipse intersecting the wellbore with a fracture width w_f at wellbore, which is much smaller than the wellbore diameter. In the elliptic coordinates, the surface of the elliptical-shape fracture is represented by the ellipse $\xi = \xi_1$, with ξ_1 being a small number. The Cartesian coordinates (x, y) and the elliptic coordinates (ξ, η) are related by $x = L\cosh\xi\cos\eta$, $y = L\sinh\xi\sin\eta$, with L being essentially the fracture half-length, and $L \gg w_f$. Subscript "f" is used for fracture quantities. The permeabilities in the reservoir and the hydraulic fracture are k, k_f, respectively, with $k \ll k_f$. The dimensionless elliptical fracture conductivity $F_E = k_f w_f/(kL)$ is related to the rectangular fracture conductivity C_{fD} by $C_{fD} = \pi F_E/4$ (Prats, 1961).

The reservoir initial pressure $P_{i,d}$ and the pressure diffusion time scale are selected as the characteristic pressure and characteristic time for non-dimensionalization: $P_c = P_{i,d}$, $t_c = \mu\varphi c_t L^2/k$, where μ, φ are the fluid viscosity and reservoir porosity, respectively. The dimensionless time $t_{DL} = tk/(\mu\varphi c_t L^2)$. The dimensionless pressure drawdown at the well P_{wD} and the dimensionless production-rate q_D are defined as:

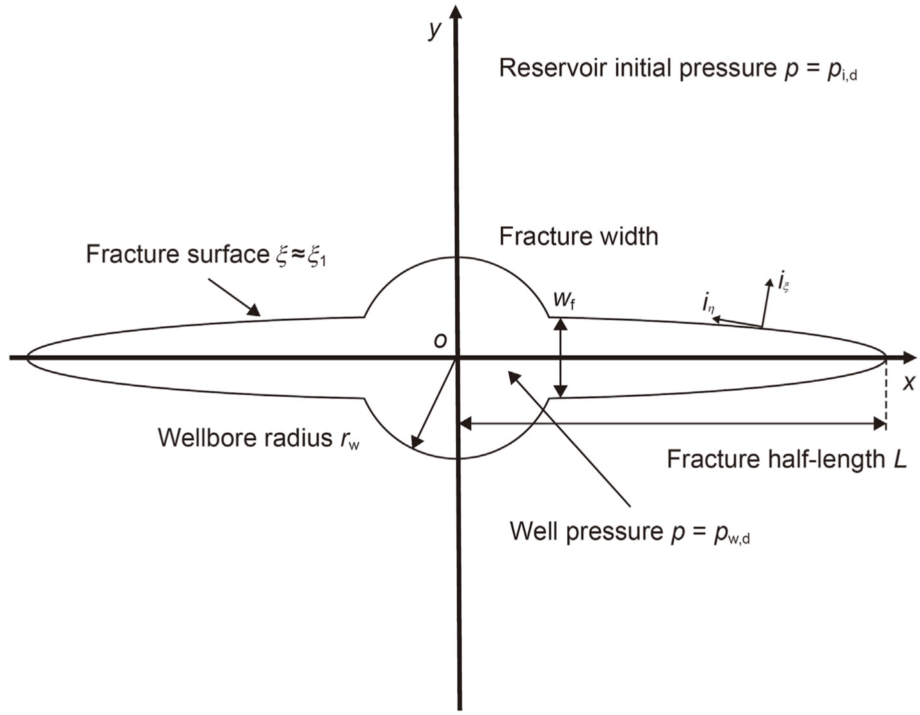

Fig. 1. Top view of a vertical well intersected by an elliptical fracture. The drawing is for illustration purpose only and it does not reflect the actual scales. In practice, the fracture is very thin and long, $L \gg w_f, \xi_1 \approx 0$.

$$p_{wD} = \frac{2\pi\kappa h \Delta p}{\mu q_d} \tag{1}$$

$$q_D = \frac{\mu q_d}{2\pi\kappa h \Delta p} \tag{2}$$

Respectively, where $\Delta P = P_{i,d} - P_{w,d}$ is the dimensional well pressure drawdown ; q_D is the dimensional production-rate at the well, and h is the height of the vertical fracture. Subscript "ST" is used for short-time solutions. For a constant-rate production, the pressure drawdown at the wellbore in short-times is given by Eq. (30) in Jin (Jin et al., 2015a):

$$p_{wD,ST} = \frac{\pi}{\sqrt{2}} \frac{1}{\Gamma(5/4)} \frac{T^{1/4}}{F_E} + \left[\frac{1}{2\sqrt{\pi}} + I(T)\right] \frac{T^{1/2}}{F_E} - \frac{2\sqrt{2\pi}\pi^2 - 1}{8\sqrt{2}\pi} \frac{1}{\Gamma(7/4)} \frac{T^{3/4}}{F_E} \tag{3}$$

with

$$I(T) = \frac{1}{3^{1/6}\pi\ \Gamma(2/3)} \left[1 - \frac{4}{\pi} \int_0^\infty \frac{\sin x}{x} \exp\left[-\left(\frac{3}{2\pi}\right)^4 T x^4 - x\right] dx\right] \tag{4}$$

$$T = F_E{}^2 t_{DL} \tag{5}$$

Γ is the Gamma function. The fracture linear flow period which precedes the bilinear flow regime has been neglected in the above short-time analysis, as is commonly adopted (Cinco-Ley and Samaniego, 1981). For the fracture linear flow, $P_{wD} \propto t_{DL}^{1/2}$ and $q_D \propto t_{DL}^{-1/2}$, which ensures that the production-rate is integrable. Thus, the short-time solution (3) starts from the bilinear flow regime, with $P_{wD} \propto t_{DL}^{1/4}$, and it extends to the formation linear flow regime which has $P_{wD} \propto t_{DL}^{1/2}$ (the second term).

An approximate steady-state flow solution was also obtained by Jin (Jin et al., 2015a, 2015b). The advantage of this approximate solution is that it is expressed in terms of elementary functions instead of special functions as in Prats (1961). In the elliptic coordinates, the outer boundary is an ellipse $\xi = \xi_e$, confocal with the limiting ellipse $\xi = \xi_1$ used to represent the fracture. The pressure on this outer boundary is $P_{e,d}$ (which is set to the initial reservoir pressure $P_{i,d}$). Subscript "SS" is used to stand for this approximate steady-state elliptical flow solution. The dimensional steady-state production-rate is given by Eq. (21) in Jin (Jin et al., 2015b):

$$q_{d,SS} = \frac{2\pi\kappa h}{\mu} \frac{\Delta p}{\xi_e - \xi_1 + \frac{1}{F_E}\left[\frac{\pi^2}{6} - \sum_{n=1}^{\infty} \frac{1}{n^2} \frac{1}{1 + nF_E \tanh 2\,n(\xi_e - \xi_1)}\right]} \tag{6}$$

From Eq. (1) and Eq. (2), the dimensionless production-rate and the dimensionless pressure drawdown at the well are then given by:

$$q_{D,SS} = \frac{1}{\xi_e - \xi_1 + \frac{1}{F_E}\left[\frac{\pi^2}{6} - \sum_{n=1}^{\infty} \frac{1}{n^2} \frac{1}{1 + nF_E \tanh 2\,n(\xi_e - \xi_1)}\right]} \tag{7}$$

$$p_{wD,SS} = \xi_e - \xi_1 + \frac{1}{F_E}\left[\frac{\pi^2}{6} - \sum_{n=1}^{\infty} \frac{1}{n^2} \frac{1}{1 + nF_E \tanh 2\,n(\xi_e - \xi_1)}\right] \tag{8}$$

Obviously, for steady-state flows, $P_{wD,SS} = 1/q_{D,SS}$. For steady-state solution, the zero-pressure-drawdown boundary is located on the outer boundary, $\xi = \xi_e$.

3. Model and results

3.1. Mathematical model

3.1.1. Mathematical model of boundary conditions

For tight gas reservoirs, diffusion of pressure disturbance is extremely slow. The zero-pressure-drawdown boundary separates the perturbed region, where there is motion of the gas, from the unperturbed region where the gas is still at rest. Since the pressure diffuses very slowly, this zero-pressure-drawdown boundary moves very slowly outwards. Within the perturbed region, the flow can be approximated as if the zero-pressure-drawdown boundary is "frozen". This type of approximation for modeling a moving boundary problem has been used in fluid mechanics as well as in crystal growth studies (Nishinaga, 2015). Furthermore, the location of zero-pressure-drawdown boundary can be found, as shown below.

Hantush & Thomas considered constant-rate groundwater production from an infinitesimal well in an anisotropic and infinite reservoir (Hantush and Thomas, 1966). They obtained the following formula for the pressure drawdown at any location $s(x,y,t) = P_i - P(x,y,t)$:

$$s(x,y,t) = \frac{Q}{4\pi T_e} W\left[\frac{S}{4t}\left(\frac{x^2}{T_x}+\frac{y^2}{T_y}\right)\right] \tag{9}$$

where Q, S are the production-rate and the storage coefficient, respectively; T_x, T_y are the two principal transmissivities with the principal axes coinciding with the x- and y-axes, respectively; $T_e = \sqrt{T_x T_y}$; and the well function $W(u)$ is given by

$$W(u) = \int_u^\infty \frac{e^{-\omega}}{\omega} d\omega = -E_i(-u) \tag{10}$$

where E_i is the exponential integral. The storage coefficient S is related to the pressure diffusion coefficient D by the relation $S = 1/D$.

Eq. (9) shows that the constant pressure drawdown lines (or isobars) are ellipses:

$$\frac{x^2}{T_x}+\frac{y^2}{T_y} = \text{const}. \tag{11}$$

In particular, the zero-pressure-drawdown boundary is given by $s(x,y,t) = 0$ which is an ellipse. Physically, this critical ellipse corresponds to the "radius of influence" for the case of an isotropic reservoir was discussed by Charbeneau (2000). Charbeneau (2000) approximated the well function $W(u)$ by the two-term expansion formula (the Jacob approximation):

$$W(u) \approx -\gamma - \ln(u) = \ln\left(\frac{e^{-\gamma}}{u}\right) = \ln\left(\frac{0.561}{u}\right) \tag{12}$$

where γ = Euler constant = 0.5772. Thus, the approximate location of the zero-pressure-drawdown boundary is

$$u = 0.561 \tag{13}$$

It is very important to note that the "radius of influence" given by Eq. (13) is independent of the rate of production Q, or equivalently the well pressure-drawdown. This is a unique property for linear problems.

From Eq. (9) and Eq. (13), the zero pressure-drawdown ellipse is given by

$$u = \frac{S}{4t}\left(\frac{x^2}{T_x}+\frac{y^2}{T_y}\right) = 0.561 \tag{14}$$

which can be re-arranged as Eq. (15):

$$\frac{x^2}{T_x\frac{2.244t}{S}}+\frac{y^2}{T_y\frac{2.244t}{S}} = 1 \tag{15}$$

In the problem of Hantush & Thomas (Hantush and Thomas, 1966), the well is infinitesimally small; and it is the anisotropy of the reservoir that causes the isobars to be elliptical. Since flow in an anisotropic reservoir is equivalent to flow induced by an elliptical fracture (Kucuk and Brigham, 1979), we can also use Eq. (15) to define the zero-pressure-drawdown isobar for fluid production from an elliptical fracture. The "anisotropy" in this case is due to the initial condition that the isobar must grow from an initially elliptical shape of the fracture surface instead of a point.

Ellipses confocal with the fracture satisfy Eq. (16):

$$\frac{x^2}{L^2\cosh^2\xi}+\frac{y^2}{L^2\sinh^2\xi} = 1 \tag{16}$$

A comparison between Eq. (15) and Eq. (16) shows that we can set the major and minor semi-axes of the zero-pressure-drawdown ellipse as

$$a_e^2 = L^2\cosh^2\xi_e = T_x\frac{2.244t}{S} \quad b_e^2 = L^2\sinh^2\xi_e = T_y\frac{2.244t}{S} \tag{17}$$

The reservoir is isotropic in the case to be studied, $T_x = T_y = 1$. As commented above, the zero-pressure-drawdown ellipse must grow from the initial ellipse used to model the fracture, instead of the origin as in the case of an infinitesimal well considered by Hantush and Thomas (1966). Thus, the initial major and minor semi-axes at $t = 0$ are

$$a_0 = L\cosh\xi_1 \approx L \quad b_0 = L\sinh\xi_1 \approx L\xi_1 \tag{18}$$

Incorporating the initial condition $t = 0: \ a_e = a_0, \ b_e = b_0$ to Eq. (17) with $T_x = T_y = 1$ leads to Eq. (19) for the zero-pressure-drawdown boundary:

$$a_e^2 = L^2\cosh^2\xi_e = L^2 + \frac{2.244t}{S}$$

$$a_e^2 = L^2\cosh^2\xi_e = L^2\xi_1^2 + \frac{2.244t}{S} \tag{19}$$

Replacing the storage coefficient by the pressure diffusivity $D = k/(\varphi\mu c_t)$, we then obtain

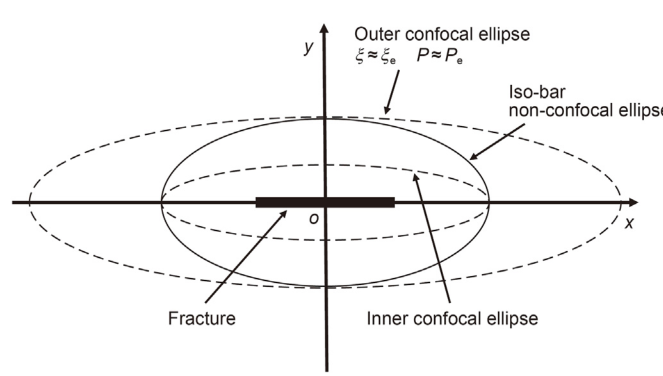

Fig. 2. Transient elliptical flow with an outward moving zero-pressure-drawdown elliptical isobar bounded by two confocal ellipses.

$$a_e^2 = L^2 \cosh^2 \xi_e = L^2 \left(1 + 2.244 \frac{D}{L^2} t\right) a_e^2 = L^2 \cosh^2 \xi_e = L^2 \left(\xi_1^2 + 2.244 \frac{D}{L^2} t\right) \tag{20}$$

Thus, in the elliptical coordinates, the zero-pressure-drawdown boundary which is a confocal ellipse, is given by the solution of ξ_e from Eq. (20):

$$\xi_e(t_{DL}) = \sinh^{-1}\left(\sqrt{\xi_1^2 + 2.244 t_{DL}}\right) = \ln\left[\sqrt{\xi_1^2 + 2.244 t_{DL}} + \sqrt{1 + \xi_1^2 + 2.244 t_{DL}}\right] \tag{21}$$

where $t_{DL} = \frac{Dt}{L^2} = tk/(\mu\varphi c_t L^2)$.

3.1.2. A new approximate solution for transient elliptical flow

The zero-pressure-drawdown isobar for a transient elliptical flow at a finite fracture conductivity is an ellipse, but not a confocal ellipse (Fig. 2). However, we use the confocal ellipse Eq. (21) as a geometric approximation to the non-confocal zero-pressure-drawdown ellipse whilst constructing the solution to a transient elliptical flow at a finite fracture conductivity. While an estimate of the error introduced by this geometric approximation is difficult to obtain, the success of this approximation is ultimately judged by the error of the solution for the pressure drawdown which can be assessed by comparison with the known solution (Section 3.3).

With the "frozen" boundary approach mentioned above (Jin et al., 2015a), an approximate well pressure drawdown P_{wD} for the transient elliptical flow can be obtained by replacing the outer pressure boundary ξ_e in the steady-state solution Eq. (8) by the time-dependent zero-pressure-drawdown boundary given by Eq. (21) for $\xi_e(t_{DL})$:

$$p_{wD,TE} = \xi_e(t_{DL}) - \xi_1 + \frac{1}{F_E}\left[\frac{\pi^2}{6} - \sum_{n=1}^{\infty} \frac{1}{n^2} \frac{1}{1 + nF_E \tanh 2\, n((t_{DL}) - \xi_1)}\right] \xi_e(t_{DL}) = \ln\left[\sqrt{\xi_1^2 + 2.244 t_{DL}} + \sqrt{1 + \xi_1^2 + 2.244 t_{DL}}\right]. \tag{22}$$

The approximate solution for transient elliptical flow Eq. (22) has some interesting properties. Since ξ_1 is very small, for large times, $t_{DL} \to \infty$, we have

$$\xi_e \to \frac{1}{2}(\ln t_{DL} + 2.194554) \tag{23}$$

If the fracture conductivity is also large, $F_E \gg 1$, then for large times, Eq. (22) and Eq. (23) give

$$p_{wD,TE} \approx \xi_e \approx \frac{1}{2}(\ln t_{DL} + 2.194554) \tag{24}$$

This is nearly identical to the result of Kucuk & Brigham (Kucuk and Brigham, 1979) for $F_E \to \infty$, $t_{DL} \to \infty$ for pseudo-radial flow:

$$p_{wD,TE} \approx \frac{1}{2}(\ln t_{DL} + 2.19537) \tag{25}$$

Thus, the transient elliptical flow solution Eq. (22) can be used for late-time pseudo-radial flow as well, which is characterized by the $lnt_{DL}/2$ behavior. Also, this is expected given that the zero-pressure-drawdown boundary grows into a circle in large times, $a_e = b_e$, from Eq. (22) for large times.

It is also worthwhile to examine the behavior of the approximate solution for transient elliptical flow Eq. (22) in short-times. For short-times, $t_{DL} \to 0$,

$$\xi_e \to \sqrt{2.244 t_{DL}} \tag{26}$$

Thus, for large fracture conductivity, $F_E \to \infty$, the well pressure drawdown from Eq. (22) becomes

$$p_{wD,TE} \approx \xi_e \approx \sqrt{2.244 t_{DL}} \tag{27}$$

This result differs slightly from the exact solution of Gringarten & Ramey (Gringarten and Ramey, 1974) for $F_E \to \infty$, $t_{DL} \to 0$:

$$p_{wD} = \sqrt{\pi t_{DL}} \tag{28}$$

This quantitative difference, however, is not surprising, since our finite fracture conductivity solution Eq. (22) is for elliptical flows, and it is not intended for use for very short-times, as the short-time solution should be provided by the asymptotic solution given in Section 2. Nevertheless, the fact that our approximate transient elliptical solution Eq. (22) can even capture the square-root of time behavior in short-times is a positive feature of this solution.

3.2. Model solution

The short-time asymptotic solution in Section 2 and the new approximate transient elliptical flow solution in Section 3.1.2 can be patched together to form a composite solution applicable to a wider range of times and flow regimes. It is noted that we only need to keep the leading terms in the short-time solution Eq. (3) up to $t_{DL}^{1/2}$, as the transient elliptical flow solution Eq. (22) also contributes at order $t_{DL}^{1/2}$. Thus, we can neglect the function $I(T)$ in the square-bracket in Eq. (3), as $I(T) = 0$ and it is of a higher order compared to the other term, $1/2\sqrt{\pi} = 0.2821$, in the same bracket.

The following observations made by Cinco-Ley & Samaniego (Cinco-Ley and Samaniego, 1981) will also be incorporated into the construction of the composite approximate solution:

(i) The bilinear flow represented by the term $t_{DL}^{1/4}$ ends at $t_{DL} = 0.1/F_E^2$ when $F_E \geq 3$;

(ii) The formation linear flow represented by the term $t_{DL}^{1/2}$ starts at $t_{DL} = 100/C_{fD}^2$ when $F_E \geq 20\pi = 62.8$, and ends at $t_{DL} = 0.016$.

Observation (i) allows us to truncate the bilinear flow contribution at $t_{DL} = 0.1/F_E^2$. Observation (ii) is reconciled with the short-time solution Eq. (3), which shows that the term $t_{DL}^{1/2}$ shows up even before $t_{DL} = 1/F_E^2$, way ahead of $t_{DL} = 100/F_E^2$. Thus, we will keep the $t_{DL}^{1/2}$ term from $t_{DL} = 0$ till $t_{DL} = 0.016$ when $F_E \geq 20\pi = 62.8$.

With these considerations in mind, a composite transient solution is constructed from Eq. (3) and Eq. (22), with the use of smoothed step functions to patch the different solutions:

$$p_{wD} = \frac{2.45083}{\sqrt{F_E}} t_{DL}{}^{\frac{1}{4}} f_-\left(t_{DL} - \frac{0.1}{F_E{}^2}\right)$$

$$+0.2821\ \ t_{DL}{}^{\frac{1}{2}}\ f_-(t_{DL} - 0.016) \times f_+(F_E - 62.8)$$

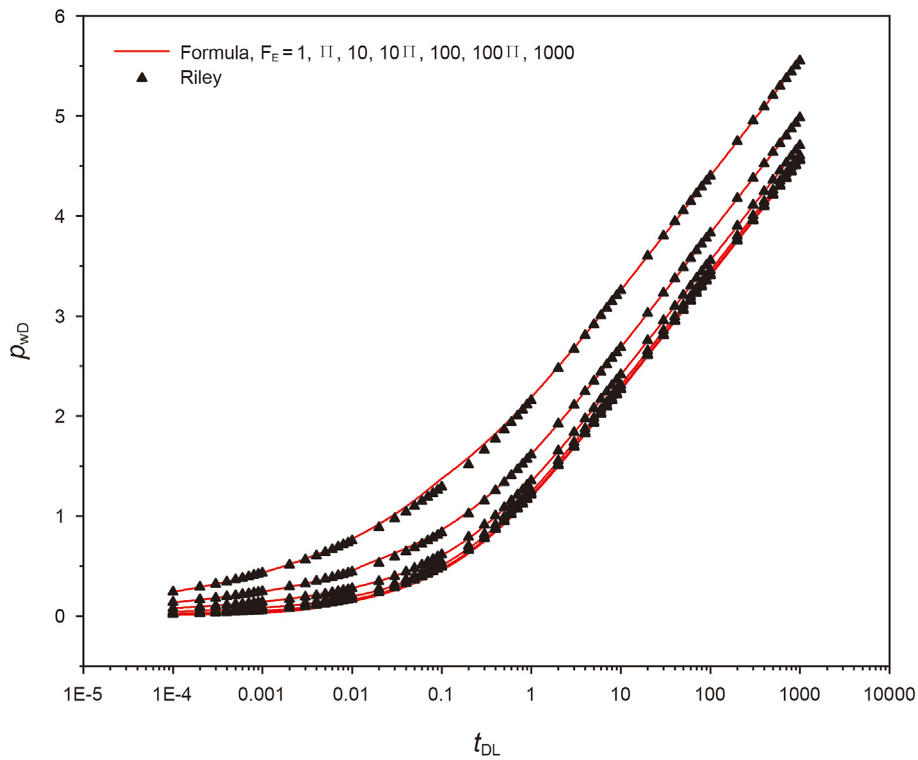

Fig. 3. With $F_E$values ranging from 0.1π to 1000, the trend curve of dimensionless pressure drawdown P_{wD} with dimensionless time t_{DL}.

$$+\left\{\xi_e(t_{DL})+\frac{1}{F_E}\left[\frac{\pi^2}{6}-\sum_{n=1}^{\infty}\frac{1}{n^2}\frac{1}{1+nF_E\tanh 2n\xi_e(t_{DL})}\right]\right\}f_+\left(t_{DL}-0.1\Big/F_E{}^2\right) \tag{29}$$

where

$$\xi_e(t_{DL})=\ln\left[\sqrt{\xi_1^2+2.244t_{DL}}+\sqrt{1+\xi_1^2+2.244t_{DL}}\right] \tag{30}$$

and the smoothed step-functions (logistic functions) are given by

$$f_-(t_{DL}-a)=\frac{1-\tanh[b(t_{DL}-a)]}{2},\ f_+(t_{DL}-a)=\frac{1+\tanh[b(t_{DL}-a)]}{2}. \tag{31}$$

In Eq. (31), b is a large constant; one can use $b = 200$, for example. For $F_E\to\infty$, and $t_{DL}\to 0$, the composite solution Eq. (29) gives $P_{wD} = 1.7801t_{DL}^{1/2}$, which is very close to the exact solution of Gringarten (Gringarten and Ramey, 1974), $P_{wD} = \sqrt{\pi}t_{DL}^{1/2} = 1.7725t_{DL}^{1/2}$.

3.3. Verification and discussion

Riley's thesis (1991) has been regarded as the most analytical, accurate and extensive study on transient flows for an elliptical fracture and it has been served as a benchmark for many subsequent works (Riley, 1991; Riley et al., 1991). The tabulated data provided in Riley's thesis (Table D1, D2 in Riley's thesis) covers seven decades of dimensionless time, t_{DL} from 10^{-4} to 10^3, with dimensionless fracture conductivity F_E values ranging from 0.1π to 1000. Our approximate analytical solution Eq. (29) for P_{wD} is compared to these tabulated data with semi-log plots in Fig. 3. In the computations, $b = 200$, $\xi_1 = 0.0001$ are used for formula Eq. (29). It is reminded that our approximate analytical solution Eq. (29) is valid for $F_E \geq 1$, which is an assumption used in Jin (Jin et al., 2015a) to derive the approximate steady-state solution. Results computed from Eq. (29) are the solid lines labeled as "formula" and those from Riley are marked by symbols.

For the pressure drawdown P_{wD}, the analytical solution Eq. (29) performed very well in the entire time range for $F_E \geq 1$, as shown in Fig. 3. Except a few points in the region transitioning from the short-time asymptotic solution Eq. (3) to the transient elliptical flow solution Eq. (22), the error remains under 1%. These comparisons over four decades of time provide validations as well as conditions for the use of the composite approximate solution Eq. (29) for transient flows in vertically fractured wells from bilinear flow regime to pseudo-radial flow regime.

The simplicity of the analytical solution Eq. (29) allows the well pressure drawdown formula to be implemented in a spreadsheet, such as Excel, even on a hand-held advanced calculator, thus providing a mobile reliable engineering tool for rapid evaluation of the transient well pressure response.

Table 1
The basic parameters of Kes2 Well from the Keshen2 Block of Tarim Oilfield.

Parameters	Symbols	Units	Value
Initial fluid pressure	$P_{i,d}$	MPa	117
Bottom hole pressure	$p_{w,d}$	MPa	61
Gas viscosity	μ	μPa•s	39.36
Fractured reservoir permeability	k	D	0.02143
Formation thickness	h	m	88.3
Production rate	q_d	m^3/d	300000
Dimensionless production index	J_D	/	0.325551

4. Case study

In this part, a field case of fractured vertical well from the Keshen Block of Tarim Oilfield from China is selected to demonstrate the model reliability and applicability.

4.1. Background

Kes2 Well is a typical fractured vertical well from the Cretaceous Bashijiqike Formation in the Keshen 2 block of Tarim Oilfield. The sandstone matrix porosity of the block is mainly distributed in 2–6%, with an average of 4.2%, and the matrix permeability is mainly distributed in $(0.01-0.5)\times 10^{-3}\,\mathbf{\mu m}^2$, with an average of $0.075\times 10^{-3}\,\mathbf{\mu m}^2$, generally belonging to ultra-low porosity, low-permeability-ultra-low permeability reservoir. Fractures in the formation of Kes2 Well are relatively developed, mainly with semi-filled high-angle fractures. At the same time, the development of tectonic fractures has the characteristics of segmented distribution, mainly with high-angle semi-filling. The buried depth is between 6570 and 6780 m. Kes2 Well was put into production in 2013. After fracturing, the daily gas production had stabilized at about 215,000 m^3/day. The testing data comes from the daily gas production and bottom hole pressure during a period of time after the well has been stably put into production after fracturing. The basic parameters of Kes2 Well have been provided in Table 1.

4.2. Model application

From Eq. (1) and $\Delta P = P_{\mathrm{i,d}} - P_{\mathrm{w,d}}$, the calculation formula of bottom hole pressure can be obtained as:

$$p_{\mathrm{w,d}} = p_{\mathrm{i,d}} - \frac{\mu q_{\mathrm{d}} p_{\mathrm{wD}}}{2\pi kh} \tag{32}$$

Under pseudo-steady-state flow, the formula of dimensionless production index is:

$$J_{\mathrm{D}} = \frac{\mu Q}{2\pi kh\left(\overline{p} - p_{\mathrm{w,d}}\right)} \tag{33}$$

Then the production formula can be expressed as:

$$Q = \frac{2\pi kh J_{\mathrm{D}}\left(\overline{p} - p_{\mathrm{w,d}}\right)}{\mu} \tag{34}$$

where:

$$\overline{p} = \frac{p_{\mathrm{i,d}} + p_{\mathrm{w,d}}}{2} \tag{35}$$

We compiled the analytical solution Eq. (29), Eq. (32) and Eq. (34) into the program. The relevant characteristic parameters of the reservoir are the input parameters. Then we obtained the data and plots of dimensionless time, t_{DL} and dimensionless pressure drawdown, p_{wD} and bottom hole pressure, $p_{\mathrm{w,d}}$ and daily gas production, Q.

In view of the large time span of a single statistical result of the existing field data (one count per day), it is not easy to obtain the statistical relationship between the dimensionless time and the dimensionless bottom hole pressure. Therefore, we use Eq. (29) to obtain the relationship between dimensionless time and daily gas production. After performing a series of type-curve matches, the best match between calculated results and field data is obtained, as shown in Fig. 4 and Fig. 5. Fig. 4 shows the relationship between the daily gas production and the dimensionless time of Kes2 Well under the analytical solution Eq. (29). It can be seen that after a period of time, the daily gas production has stabilized at about 220,000 m^3/day. Fig. 5 shows the comparison of field data and calculation results of analytical model Eq. (29) with daily gas production as the abscissa and bottom hole pressure as the ordinate. These results are basically consistent with the overall understanding of Kes2 Well in the Keshen2 Block of Tarim Oilfield. It is

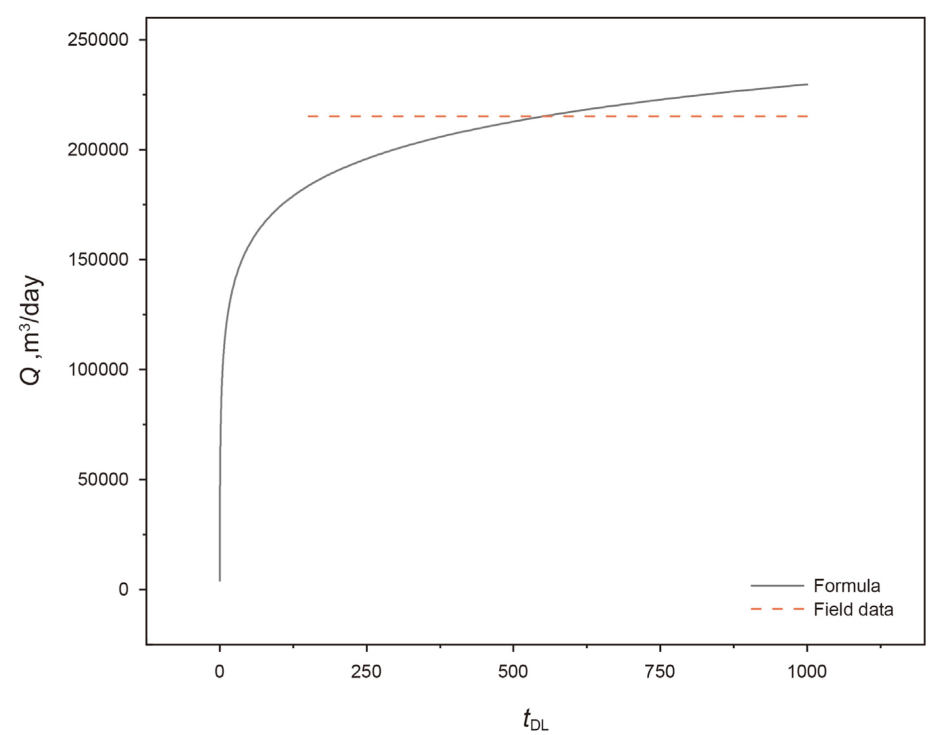

Fig. 4. The relationship between the daily gas production and the dimensionless time of Kes2 Well under the analytical solution.

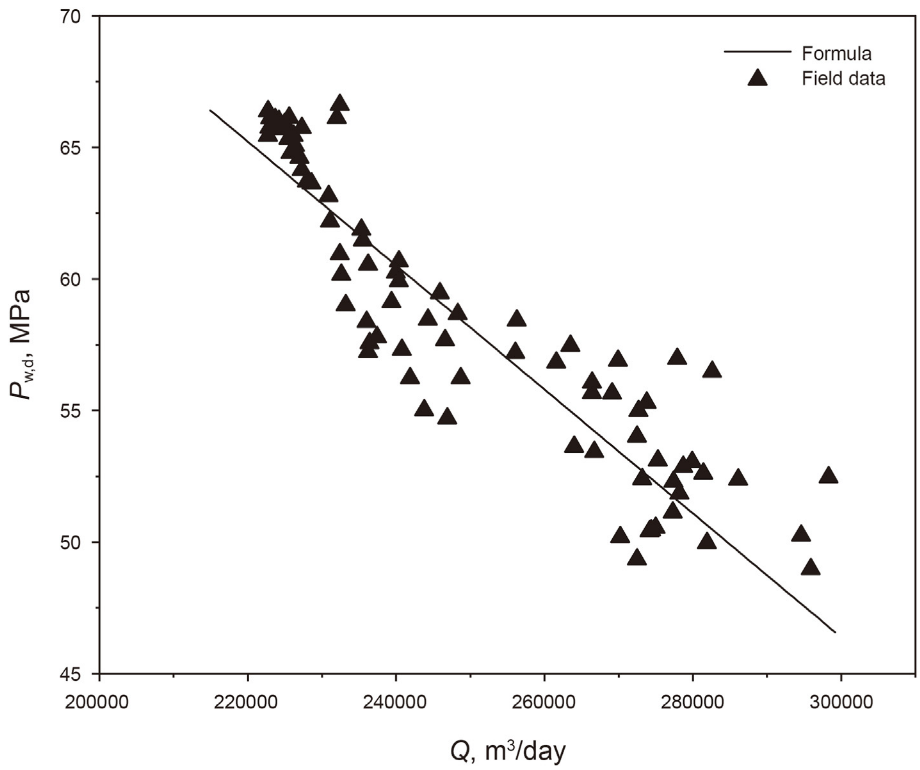

Fig. 5. The comparison of field data and calculation results of analytical solution.

very convenient for evaluating fracture conductivity and production after hydraulic fracturing in the field.

5. Conclusions

This work presents an approximate analytical solution Eq. (29) for transient flow during constant-rate production from a vertically-fractured well in an infinite homogeneous reservoir with finite fracture conductivity. The solution covers transient flows from the bilinear flow regime to the pseudo-radial flow regime. The solution for the pressure drawdown shows excellent agreement with the results of Riley (1991) over seven decades of time when $F_E \geq 1$. The explicit real-time well pressure drawdown analytical model can be easily implemented in a spread sheet such as Excel, even on a hand-held calculator, thus serving as a practical and reliable engineering tool for rapid evaluation of the transient well pressure response.

Declaration of competing interest

The authors declare no conflict of interest.

Acknowledgments

This work is supported by the Chinese National Natural Science Foundation Grant 52074314.

References

Agarwal, R.G., Carter, R.D., Pollock, C.B., 1979. Evaluation and performance prediction of low-permeability gas wells stimulated by massive hydraulic fracturing. J. Petrol. Technol. 31 (3), 362–372. https://doi.org/10.2118/6838-PA.

Agarwal, R.G., 1980. A new method to account for producing time effects when drawdown type curves are used to analyze pressure buildup and other test data. SPE Annual Technical Conference and Exhibition, Dallas, the USA. https://doi.org/10.2118/9289-MS, 21-24 September.

Amini, S., Ilik, D., Blasingame, T.A., 2007. Evaluation of the elliptical flow period for hydraulically-fractured wells in tight gas sands-theoretical aspects and practical considerations. In: SPE Hydraulic Fracturing Technology Conference, vols. 29–31. the U.S.A. https://doi.org/10.2118/106308-MS. College Station, Texas.

Baker, B.J., Ramey Jr., H.J., 1978. Transient Flow to Finite Conductivity Vertical Fractures. Annu. Tech. Conf. Exhib., Houston, TX https://doi.org/10.2118/7489-MS. SPE 7489.

Biryukov, D., Kuchuk, F.J., 2012. Transient pressure behavior of reservoirs with discrete conductive faults and fractures. Transport Porous Media 95, 239–268. https://doi.org/10.1007/s11242-012-0041-x.

Blasingame, T.A., 2008. The Characteristic Flow Behavior of Low-Permeability Reservoir Systems. SPE Unconventional Reservoirs Conference. https://doi.org/10.2118/114168-MS. Keystone, CO, USA, Feb.

Charbeneau, R.J., 2000. Groundwater Hydraulics and Pollutant Transport. Prentice Hall, Upper Saddle River, N.J.

Chen, K.P., 2016. Production from a fractured well with finite fracture conductivity in a closed reservoir: an exact analytical solution for pseudo-steady state flow. SPE J. 21 (2), 550–556. https://doi.org/10.2118/179739-PA.

Chen, Z.M., Liao, X.W., Zhao, X.L., Dou, X.J., Zhu, L.T., 2016. A semi-analytical mathematical model for transient pressure behavior of multiple fractured vertical well in coal reservoirs incorporating with diffusion, adsorption, and stress-sensitivity. J. Nat. Gas Sci. Eng. 29, 570–582. https://doi.org/10.1016/j.jngse.2015.08.043.

Cinco-Ley, H., Meng, H., 1988. Pressure Transient Analysis of Wells with Finite-Conductivity Vertical Fractures in Double-Porosity Reservoirs. SPE Annual Technical Conference and Exhibition, Houston, Texas, the USA. https://doi.org/10.2118/18172-MS. SPE 18172.

Cinco-Ley, H., Samaniego, V.F., Dominguez, A.N., 1978. Transient pressure behavior for a well with a finite-conductivity vertical fracture. SPE J. 18 (4), 253–264. https://doi.org/10.2118/6014-PA.

Cinco-Ley, H., Samaniego, V.F., 1981. Transient pressure analysis for fractured wells. J. Petrol. Technol. 33 (9), 1749–1766. https://doi.org/10.2118/7490-PA.

Gringarten, A.C., Ramey Jr., H.J., 1974. Unsteady pressure distribution created by a well with a single infinite-conductivity vertical fracture. SPE J. 14, 347–360. https://doi.org/10.2118/4051-PA.

Gringarten, A.C., Ramey Jr., H.J., Raghavan, R., 1975. Applied pressure analysis for fractured wells. J. Petrol. Technol. 27 (7), 887–892. https://doi.org/10.2118/5496-PA.

Hale, B.W., Evers, J.F., 1981. Elliptical flow equations for vertically fractured gas wells. J. Petrol. Technol. 33 (12), 2489–2497.

Hantush, M.S., Thomas, R.G., 1966. A method for analyzing a drawdown test in anisotropic aquifers. Water Resour. Res. 2 (2), 281–285. https://doi.org/10.1016/S0022-1694(67)80044-1.

Jiang, L.W., Liu, J.J., Liu, T.J., Yang, D.Y., 2020. Semi-analytical modeling of transient pressure behaviour for a fractured vertical well with hydraulic/natural fracture networks by considering stress-sensitive effect. J. Nat. Gas Sci. Eng. 82, 103477. https://doi.org/10.1016/j.jngse.2020.103477.

Jiang, R.Z., Zhang, F.L., Cui, Y.Z., Qiao, X., Zhang, C.G., 2019. Production performance analysis of fractured vertical wells with SRV in triple media gas reservoirs using elliptical flow. J. Nat. Gas Sci. Eng. 68, 102925. https://doi.org/10.1016/j.jngse.2018.01.032.

Jin, Y., Chen, K.P., Chen, M., 2015a. An asymptotic solution for fluid production from an elliptical hydraulic fracture at early-times. Mech. Res. Commun. 63, 48–53. https://doi.org/10.1016/j.mechrescom.2014.12.004.

Jin, Y., Chen, K.P., Chen, M., 2015b. Analytical solution and mechanisms of fluid production from hydraulically-fractured wells with finite fracture conductivity. J. Eng. Math. 92, 103–122. https://doi.org/10.1007/s10665-014-9754-x.

Kucuk, F., Brigham, W.E., 1979. Transient flow in elliptical systems. SPE J. 19 (6), 401–410. https://doi.org/10.2118/7488-PA.

Kuchuk, F., Habashy, T., 1997. Pressure behavior of laterally composite reservoirs. SPE Form. Eval. 12 (1), 47–56. https://doi.org/10.2118/24678-PA.

Lee, W.J., Holditch, S.A., 1981. Fracture evaluation with pressure transient testing in low-permeability gas reservoirs. JPT (J. Pharm. Technol.) 1776–1792. https://doi.org/10.2118/9975-PA.

Lu, Y., Chen, K.P., 2016. Productivity index optimization for hydraulically fractured vertical wells in a circular reservoir: a comparative study using analytical solutions. SPE J. 21 (6), 2208–2219. https://doi.org/10.2118/180929-PA.

Nguyen, Kien H., Zhang, M., Ayala, Luis F., 2020. Transient pressure behavior for unconventional gas wells with finite-conductivity fractures. Fuel 266, 117119. https://doi.org/10.1016/j.fuel.2020.117119.

Nie, R.S., Fan, X.H., Li, M., Chen, Z.X., Deng, Q., Lu, C., Zhou, Z.L., Jiang, D.W., Zhan, J., 2021. Modeling transient flow behavior with the high velocity non-Darcy effect in composite naturally fractured-homogeneous gas reservoirs. J. Nat. Gas Sci. Eng. 96, 104269. https://doi.org/10.1016/j.jngse.2021.104269.

Nishinaga, T., 2015. Handbook of Crystal Growth: Volume 1 Part B, Transport and Stability. Elsevier, Amsterdam.

Obut, S.T., Ertekin, T.A., 1987. Composite system solution in elliptic flow geometry. SPE Form. Eval. 2, 227–238. https://doi.org/10.2118/13078-PA.

Poston, S.W., Poe, B.D., 2008. Analysis of Production Decline Curves. Richardson, TX.

Prats, M., 1961. Effect of vertical fractures on reservoir behavior—incompressible fluid case. SPE J. 1 (2), 105–118. https://doi.org/10.2118/1575-G.

Prats, M., Hazebroek, P., Strickler, W.R., 1962. Effect of vertical fractures on reservoir behavior-compressible fluids case. SPE J. 2 (2), 87–94. https://doi.org/10.2118/98-PA.

Raghavan, R., 1977. Pressure Behavior of Wells Intercepting Fractures. Proc. Invitational Well Testing Symposium, Berkeley, CA, pp. 19–21.

Riley, M.F., 1991. Finite Conductivity Fractures in Elliptical Coordinates. Ph.D. Dissertation, Stanford Univ., Stanford, CA.

Riley, M.F., Horne, R.N., Brigham, W.E., 1991. Analytic Solutions for Elliptical Finite Conductivity Fractures. SPE Annual Technical Conference and Exhibition, Dallas, Texas, the USA. https://doi.org/10.2118/22656-MS. SPE 22656.

Rushing, J.A., Blasingame, T.A., 2003. Integrating Short-Term Pressure Transient Testing and Long-Term Production Data Analysis to Evaluate Hydraulically-Fractured Gas Well Performance. Annual SPE Technical Conference and Exhibition. https://doi.org/10.2118/84475-MS. Denver, CO., 05-08 October, SPE 84475.

Russell, D.G., Truitt, N.E., 1964. Transient pressure behavior in vertically fractured reservoirs. J. Petrol. Technol. 1159–1170. https://doi.org/10.2118/967-PA.

Sun, H., Ning, Z., Yang, X., Jin, Y., Lu, Y., Chen, K.P., 2017. An analytical solution for pseudosteady state flow in a hydraulically-fractured stratified reservoirs with interlayer crossflows. SPE J. 22 (4), 1103–1111. https://doi.org/10.2118/185163-PA.

Tian, F., Du, X.K., Wang, X.D., Xu, W.L., 2018. Rate decline analysis for finite conductivity vertical fractured gas wells produced under a variable inner boundary condition. J. Petrol. Sci. Eng. 171, 1249–1259. https://doi.org/10.1016/j.petrol.2018.08.060.

Valko, P., Economides, M.J., 1997. Transient behavior of finite conductivity horizontal fractures. SPE J. 2, 213–222. https://doi.org/10.2118/38436-PA.

Wan, H., Ran, Q.Q., Liao, X.W., 2017. Pressure transient responses study on the hydraulic volume fracturing vertical well in stress-sensitive tight hydrocarbon reservoirs. Int. J. Hydrogen Energy 42 (29), 18343–18349. https://doi.org/10.1016/j.ijhydene.2017.04.143.

Wattenbarger, R.A., Ramey Jr., H.J., 1969. Well test interpretation of hydraulically fractured wells. J. Petrol. Technol. 625–632. https://doi.org/10.2118/2155-PA.

Wilkinson, D.J., 1989. New Results for Pressure Transient Behavior of Hydraulically-Fractured Wells. Low Permeability Reservoirs Symposium. https://doi.org/10.2118/18950-MS. SPE-18950, Denver, Colorado, the USA.

Zhang, L., Zhang, X., Wang, Y., Zhao, Y., 2011. A study on elliptical gas flow in triporosity gas reservoirs. Transport Porous Media 87, 777–791. https://doi.org/10.1007/s11242-011-9718-9.

Zhang, Q.S., Wang, X.Z., Wang, D.H., Zeng, J., Zeng, F.H., Zhang, L., 2018. Pressure transient analysis for vertical fractured wells with fishbone fracture patterns. J. Nat. Gas Sci. Eng. 52, 187–201. https://doi.org/10.1016/j.jngse.2018.01.032.